Statistical and Constraint Loss Size Effects on Cleavage Fracture–Implications to Measuring Toughness in the Transition

H. J. Rathbun[1]
e-mail: palmtree@engineering.ucsb.edu

G. R. Odette

T. Yamamoto

M. Y. He

G. E. Lucas

University of California,
Santa Barbara, CA 93106-5050

A systematic investigation of the effects of specimen size on the cleavage fracture toughness of a typical pressure vessel steel is reported. Size dependence arises both from: (i) statistical effects, related to the volume of highly stressed material near the crack tip, that scales with the crack front length (B) and (ii) constraint loss, primarily associated with the scale of plastic deformation compared to the un-cracked ligament dimension (b). Previously, it has been difficult to quantify the individual contributions of statistical versus constraint loss size effects. Thus, we developed a single variable database for a plate section from the Shoreham pressure vessel using a full matrix of three point bend specimens, with B from 8 to 254 mm and b from 3.2 to 25.4 mm, that were tested at a common set of conditions. The University of California Santa Barbara (UCSB) b-B database was analyzed using three-dimensional finite element calculation of the crack tip fields combined with a cleavage model calibrated to the local fracture properties of the Shoreham steel. This paper focuses on the possible significance of these results to the Master Curve standard as formulated in ASTM E 1921. The statistical scaling procedure to treat variations in B used in E 1921 was found to be reasonably consistent with the UCSB b-B database. However, constraint loss for three point bend specimens begins at a deformation level that is much lower than the censoring limit specified in E 1921. Unrecognized constraint loss leads to a nonconservative, negative bias in the evaluation of T_o, estimated to be typically on the order of $-10\,^{\circ}\mathrm{C}$ for pre-cracked Charpy specimens. [DOI: 10.1115/1.2217962]

Keywords: constraint effects, statistical effects, transition toughness

1 Introduction

The American Society for Testing and Materials (ASTM) E 1921, "Standard Test Method for Determination of Reference Temperature, T_o, for Ferritic Steels in the Transition Range,"[2] represents a very important advance in fracture mechanics testing [1–3]. Commonly known as the Master Curve Method, E 1921 permits establishing the entire cleavage initiation toughness-temperature master curve, $K_{mc}(T)$, based on tests using a relatively small number of relatively small single edge notched (pre-cracked) bend [SEN(B)] or compact tension [$C(T)$] specimens. The pertinent specimen dimensions are the crack depth (a), width (W), a/W ratio (≈ 0.5), un-cracked ligament length ($b=W-a$) and thickness (B). Note, a list of nomenclature used in this paper is given in the Appendix.

The Master Curve Method rests on several key assumptions that generally appear to be empirically successful. These include:

- The toughness temperature $K_{mc}(T\text{-}T_o)$ master curve has a constant, invariant shape that can be indexed on an absolute temperature, T, scale by a reference temperature, T_o, corresponding to a median toughness of 100 MPa$\sqrt{\text{m}}$.
- The T_o, as well as the mean and median toughness, can be estimated using maximum likelihood statistical methods, in some cases by testing as few as six specimens at a single temperature in the transition.
- Scatter in fracture toughness is governed by weakest link statistics, with a Weibull toughness modulus of 4. Statistical considerations can be used to set $K_{mc}(T)$ confidence bounds for a particular data set.
- The Weibull statistics apply to the distribution of (K_{Jm}-K_{min}), where K_{Jm} is the measured toughness and K_{min} is a minimum toughness for cleavage fracture. The concept of a K_{min} is based on conditional probability of fracture arguments. However, the fixed value in E 1921-97 of $K_{min}=20$ MPa$\sqrt{\text{m}}$ is essentially an empirically derived value.
- Statistical sampling size effects are associated with variations in the crack front length, B, that can be accounted for by adjusting K_{Jm} to a reference toughness, K_{Jr}, for a reference thickness, $B_r=25.4$ mm. The adjustment uses the scaling relation $K_{Jr}(B_r)=(K_{Jm}(B)-20)\times(B/B_r)^{1/4}+20$ MPa$\sqrt{\text{m}}$. Hereafter, we will refer to this as the $(B/B_r)^{1/4}$-K_{min} statistical size scaling procedure.

[1]Corresponding author, currently with University of California, Lawrence Livermore National Laboratory.

[2]The analyses contained in this publication were performed to the specifications of the 1997 edition of ASTM E 1921. The changes embodied in the 2003 edition of ASTM E 1921 do not substantially affect the conclusions of this work.

Contributed by the Pressure Vessels and Piping Division of ASME for publication in the JOURNAL OF PRESSURE VESSEL TECHNOLOGY. Manuscript received August 23, 2004; final manuscript received June 24, 2005. Review conducted by Poh-Sang Lam.

- Constraint effects[3] are treated by a deformation limit censoring procedure. Censoring specifies a maximum measurable toughness, K_{max} based on a dimensionless deformation parameter $M=E\sigma_y b/K_{Jc}^2$ exceeding a minimum value of $M_{lim}=30$, where σ_y is the yield stress, E is the modulus of elasticity and b is the in-plane ligament length. Thus, $K_{max}=\sqrt{(E\sigma_y b/30)}$. Censored data are used in the T_o analysis by assuming that $K_{Jm}=K_{max}$ if there are a sufficient number of uncensored data points.

Statistical models based on a weakest link concept, proposed by Wallin et al. [4], provided the primary theoretical framework underpinning the master curve method. Statistical models predict an inherent size effect on K_{Jc} due to variations in the highly stressed volume of material near the crack tip. For through-cracked specimens, the stressed volume varies with crack front length, B. The $(B/B_r)^{1/4}$-K_{min} statistical size scaling basically arises from the fact that the stressed volume (V) for a specified B varies with the applied loading as K_J^4. Thus, the stressed volume is the same when $K_J(B_1)/K_J(B_2)=(B_2/B_1)^{1/4}$. This relation is modified in E 1921 to account for a $K_{min}=20$ MPa$\sqrt{m}$.

However, size effects can also arise from constraint loss. Constraint loss is related to the specimen geometry and length scale of high crack tip stress fields (proportional to $K_J^2/E\sigma_y$) compared to the ligament size (b). Out-of-plane constraint loss also occurs as a function of M,B, and B/W [5–7]. For very large ratios of $b/(K_J^2/E\sigma_y)=M$, and plane strain, the fields approach an asymptotic, size-independent small scale yielding (SSY) reference condition. Constraint loss is associated with reductions in the stress and spatial amplitudes of the crack tip fields relative to the SSY reference condition at a specified K_J loading. As a consequence, the measured toughness is higher under conditions of constraint loss than for SSY.

The actual specimen geometry is important as well, primarily as it relates to nonsingular T-stresses acting in the direction of crack propagation.[4] Negative (compressive) T-stresses also cause constraint loss by reducing the magnitudes of the stress fields, even at small loading levels [5,8,9]. In contrast, positive (tensile) T-stresses, which occur in $C(T)$ specimens, actually increase the amplitudes of the stress fields. Thus, the positive T-stress makes the $C(T)$ geometry more resistant to deformation induced constraint loss compared to SEN(B) specimens [9]. As a consequence of these complexities, SSY fields occur in actual specimens only under a very limited set of conditions. Thus, we will focus our assessment of constraint loss with reference to the idealized SSY condition where the T-stresses are equal to zero. Concepts associated with quantifying and adjusting for constraint loss are discussed further in Secs. 4 and 5 below.

Most previous K_{Jc} tests with $a/W\approx 0.5$ were for B/b between 1 and 2 [10]. Since both b and B varied in the same proportion to the absolute specimen size, it has not been possible to evaluate reliably the relative contributions of the statistical versus constraint loss effects based on the previously existing data. That is, constraint loss effects could be mistaken for statistical effects. Of course, for sufficiently large specimens, with assuredly full constraint, statistical effects can be evaluated directly. However, finite element (FE) crack tip field models, using critical stress-critical stressed region or Weibull stress local cleavage criteria, indicate that constraint loss occurs at M significantly larger than 30 in SEN (B) specimens [5,10]. Further, a preliminary evaluation of statistical size effects did not clearly support the $(B/B_r)^{1/4}$-K_{min} type statistical size scaling [10]. Because of the complex assessment procedure in E 1921, including the use of censored data, the general effect of unrecognized constraint loss on T_o must be assessed on a case-by-case basis. However, data sets subject to significant constraint loss bias T_o towards the lower, nonconservative direction compared to more fully constrained conditions. Thus, key questions we address in this paper are as follows:

- Is the $(B/B_r)^{1/4}$-K_{min} statistical size scaling procedure consistent with toughness variations over a large range of B for conditions of high constraint?
- How does constraint loss vary as a function of deformation for the SEN(B) geometry?
- Is the $M_{lim}=30$ in E 1921 sufficient to avoid nonconservative bias in T_o values compared to higher constraint conditions?

In order to answer these questions, a "single variable"[5] toughness database was developed and subjected to a physically based analysis to separate and quantify both statistical and constraint mediated size effects. To this end, a matrix of fracture specimens with B from 8 to 254 mm and b from 3.2 to 25.4 mm, shown in Fig. 1, was fabricated from a single plate section of A533B steel, taken from the Shoreham reactor pressure vessel. The UCSB b-B test matrix covers a large range of specimen size and geometry. The specimens were tested at a common set of experimental conditions. The UCSB b-B database was analyzed using two types of calibrated cleavage models as discussed in [7]. This paper describes the implementation and implications of one of these models as discussed in Secs. 4 and 5 below, while the other (Weibull stress) model is discussed in more detail in [7]. Both models are based on local cleavage fracture criteria, coupled with three-dimensional (3D) FE calculations of crack tip fields. The models are used to predict the ratio of the K_J, with constraint loss (K_{CL}), that produces the same critically stressed region at the crack tip as the K_J under SSY (K_{SSY}). The $[K_{CL}/K_{SSY}]>1$ defines the "theoretical" increase in toughness due to constraint loss. The measured toughness, K_{Jm} is adjusted to a SSY K_{Jc} as $K_{Jc}=K_{Jm}/[K_{CL}/K_{SSY}]$. The adjusted K_{Jc} at various B are then used to test the validity of the $(B/B_r)^{1/4}$-K_{min} statistical size scaling procedure. Thus, combined with the model-based analysis, the single variable UCSB b-B database allows an explicit, albeit approximate, de-coupling of statistical and constraint mediated size effects.

In the remainder of this paper, we will emphasize of implications to the UCSB b-B database and model-based analysis to the Master Curve Method as formulated in ASTM E 1921. More detailed descriptions of both the experimental procedures and overall UCSB database on the Shoreham material, as well as the more fundamental insight derived from the analysis, can be found in [6,7,11,12].

In summary, we found that the $(B/B_r)^{1/4}$-K_{min} statistical size scaling procedure is reasonably consistent with the UCSB b-B database. This B-scaling is used in the remainder of this paper. After application of both the constraint loss $[K_{CL}/K_{SSY}]$ adjustment and the $(B/B_r)^{1/4}$-K_{min} statistical size scaling to a reference thickness $B_r=25.4$ mm, the resulting K_{Jr} form a reasonably homogeneous population, that is approximately independent of both specimen size and geometry. However, there are two exceptions. The $[K_{CL}/K_{SSY}]$ procedure appears to slightly over adjust the K_{Jm}

[3]Note, the Master Curve Method is explicitly for standard 1 T-(25.4 mm thick) SEN(B) and C(T) specimens as opposed to a fully constrained, plane strain SSY condition. However, at toughness levels in the range of 100 MPa$\sqrt{m}$, 1 T specimens have a relatively high level of constraint in medium-strength, pressure vessel steels.

[4]The T-stress is a component of the elastic stress tensor. Its relative importance to crack tip stress distributions increases rapidly with deformation in the elastic regime in proportion to the load. The T-stress continues to provide reasonable descriptions of deviations from SSY in the elastic-plastic regime. The T-stress is small, and thus plays a secondary role, for the deeply cracked SEN(B) specimens used in this study.

[5]In this context, single variable means that B or b was varied while all other specimen and test conditions were held constant; and that within the matrix of B variations there are b-B combinations that are not expected to manifest significant size effects due to constraint loss.

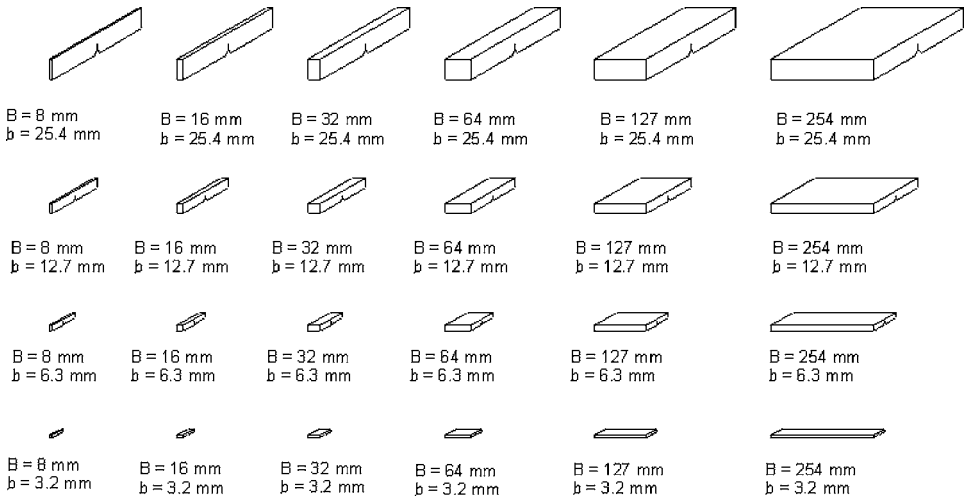

Fig. 1 Test specimen matrix. Eight tests were conducted for each specimen size and geometry.

data for two of the five B/b geometries at the smallest b. Over-adjustments result in predicted toughness values that are believed to be too low compared to the actual K_{Jc}. Further, the $(B/B_r)^{1/4}$-K_{min} statistical size scaling procedure also somewhat over adjusts the K_{Jc} data for the specimens with the largest B. These over-adjustments result in predicted toughness values that are too high compared to the actual K_{Jr}.

However, these possible "discrepancies" are fairly small, and a more significant result is that constraint loss begins at a value of M of more than 100 for SEN(B) specimens with $B/b>1$ (encompassing the typical range of test specimen geometry of 1 to 2). This M is much higher than the $M=30$ censoring limit currently used in E 1921. More detailed analysis and discussion of the separation of statistical and constraint loss mediated size scaling is given in [6,7,11].

2 Experiment

The specimen matrix, shown in Fig. 1, included variations in B for a set of constant b, and variations in b for a set of constant B. The nominal values of B and b are 8, 16, 32, 64, 127, and 254 mm, and 25.4, 12.7, 6.3, and 3.2 mm, respectively. A section of ASTM A533 Grade B Class 1 plate from the decommissioned Shoreham vessel was machined into SEN(B) specimens in the L-S orientation with span (S) to width ratio $S/W=4$ and $a/W \approx 0.5$. Individual specimen types were taken from randomized locations within the original steel plate. Fatigue pre-cracking procedures were developed to ensure an acceptably straight crack front as described in [12]. All specimens were machined and fatigue pre-cracked such that the crack tip was positioned 3/4 of the total pressure vessel thickness from the inside surface of the plate (referred to as the 3/4-T location). Pre-cracking was not successful in the case of the $B=64$ mm, $b=3.2$ mm specimens; hence, this geometry is not included in the final test matrix. Based on preliminary measurements using 1 T $C(T)$ specimens aimed at achieving a median K_{Jr} of 100 MPa$\sqrt{m}$, all quasi-static loading rate tests were carried out at −91 °C. Eight tests were carried out at each b-B matrix point. Thus, there are a total of 184 K_{Jm} data points in the UCSB b-B matrix. With only minor or necessary exceptions, including atypical specimen geometry (e.g., large and small B/b ratios), the fracture tests followed the basic ASTM E 1921-97 procedures. Fracture occurred by cleavage initiation in all cases. For $b=25.4$ mm, M is generally sufficiently large (>100) to assure relatively modest constraint loss effects in all but the thinnest specimens. In the latter case, at small B/b, the specimens rapidly lose lateral constraint. The large range of B from 8 to 254 mm produces a maximum variation in K_{Jr} of a factor of about 2 for $(B/B_r)^{1/4}$-K_{min} statistical size scaling. The large variations in b were used to explore a wide range of constraint conditions, down to M values of less than 10.

3 Experimental Data Trends

Figure 2 plots the K_{Jm} versus log B for varying b. Use of a log scale and the slight data point off-sets for different b are for the

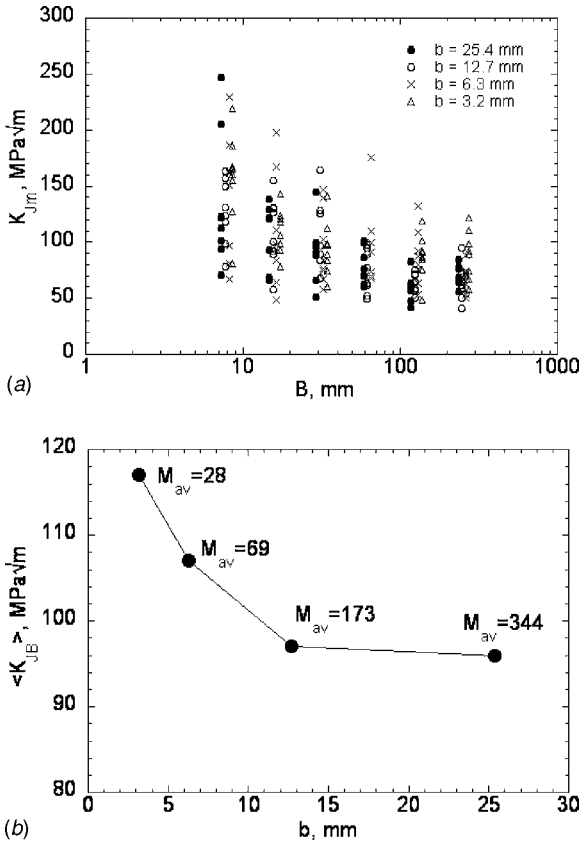

Fig. 2 (*a*) K_{Jm} versus log B for the UCSB b-B matrix in this study. The data at various b are slightly off-set in B for clarity. The solid curve is the fit to the $b=25.4$ mm data. (*b*) Averaged K_{JB} for all B grouped by common b plotted versus b.

purpose of clarity. The toughness generally decreases with increasing B, consistent with statistical size effects. A least squares fit of the mean $\langle K_{Jm}(B)\rangle$ for the largest $b=25.4$ mm ($W=50.8$ mm) specimens to

$$\langle K_{Jm}(B)\rangle = (\langle K_{Jm}(B_r)\rangle - 20)(B_r/B)^p + 20 \text{ MPa}\sqrt{\text{m}} \quad (1)$$

gives $p=0.26\pm0.09$, in almost exact agreement with the ASTM E 1921 $(B/B_r)^{1/4}$-K_{min} statistical size scaling procedure. In general, the K_{Jm} are also larger for the specimens with smaller b, due to loss of in-plane constraint. Note that, for the UCSB b-B matrix in which all specimens have $a/W\approx0.5$, in-plane constraint loss is due to the variations in the absolute b dimension. However, as seen for the $b=25.4$ mm specimens with $B=8$ mm, some K_{Jm} are also higher at the smallest B/b due to loss of out-of-plane constraint. The general trend in constraint loss is better illustrated in Fig. 2(b), plotting $\langle K_{JB}\rangle=\langle[(K_{Jm}-20)(B/B_r)^{1/4}+20]\rangle$ MPa$\sqrt{\text{m}}$ as a function of b, where $\langle K_{JB}\rangle$ is the K_{JB} averaged for all B at a given b, after adjusting K_{Jm} to the reference thickness of $B_r=25.4$ mm. For example, the data point at $b=3.2$ mm in Fig. 2(b) was calculated by adjusting all of the measured K_{Jm} from the bottom row of the b-B matrix (Fig. 1) to the reference thickness $B_r=25.4$ mm, and then averaging these adjusted values. The average values of M for the various b are also shown. Significant constraint loss is observed at the two smallest b.

These purely empirical trends demonstrate that various combinations of statistical and constraint mediated size effects occur in the b-B test matrix, consistent with the basic objectives of the experiment. However, further quantification and a rigorous decoupling of these effects requires a more detailed mechanism-based analysis.

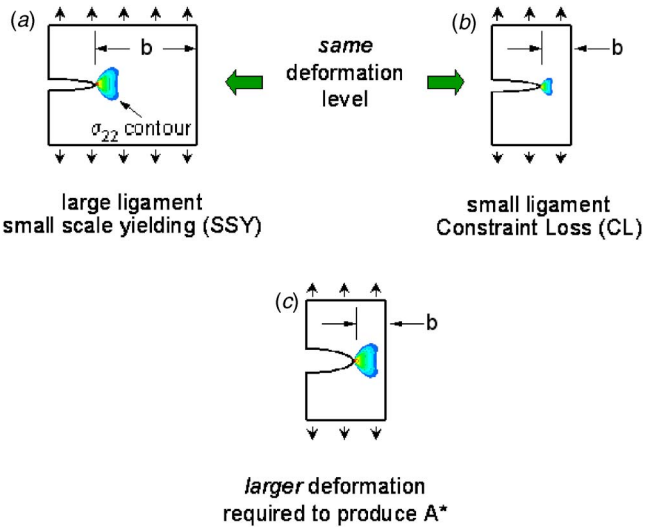

Fig. 3 A schematic illustration of the basis for constraint adjustment. Figure 3(*a*) illustrates an approximate condition of SSY. Here the high stress region, marked by the σ_{22} stress contour (not to scale), is small compared to *b*. Figure 3(*b*) shows that the $A(\sigma_{22})$ contour is smaller than in Fig. 3(*a*) if the applied K_J are the same. Figure 3(*c*) shows that to achieve the same $A(\sigma_{22})$ in smaller specimens requires a $K_{CL}>K_{SSY}$. Cleavage occurs in both cases when $A=A^*$ and $\sigma_{22}=\sigma^*$. Note, thicker specimens (larger *B*) require a smaller A^* to achieve the same V^*

4 The Mechanics of Size Effects and Finite Element Models of Constraint Loss

Three-dimensional (3D) calculations of crack tip stress and strain fields using the ABAQUS finite element (FE) software [13] were used to analyze the UCSB b-B database described in the previous section by estimating the effect of constraint loss for each K_{Jm} data point. Details of the FEA are provided in [6,7]. We followed the general approach of Nevalainen and Dodds [5] to develop what we term the $[K_{CL}/K_{SSY}]$ constraint adjustment procedure. The physical basis for $[K_{CL}/K_{SSY}]$ constraint adjustment is illustrated in Fig. 3 and can be summarized as follows:

- The basic local fracture criterion is that the normal (σ_{22}) (or alternately the principal stress) in front of a blunting crack equals a critical microcleavage fracture stress ($\sigma_{22}=\sigma^*$) over a critical microstructural volume (V^*) of material that is needed to initiate cleavage at a brittle trigger particle. For a through cracked specimen, cleavage occurs when the in-plane area, $\langle A(\sigma^*)\rangle$, equals a critical area (A^*), since $\langle A^*(\sigma^*)\rangle B=V^*$. Note that $A(\sigma^*)$ is averaged across the specimen thickness (i.e., to calculate $\langle A(\sigma^*)\rangle$) to account for out-of-plane constraint loss.
- For SSY, $\langle A(\sigma^*)\rangle$ increases with K_J^4 and cleavage occurs at $K_{SSY}=K_{Jc}$, when the $\langle A^*(\sigma^*)\rangle$ condition is achieved. However, under constraint loss, a $K_{CL}>K_{SSY}$ is needed to achieve the $A^*(\sigma^*)$. Thus, in general, $K_{Jm}/K_{Jc}\geq1$.
- Within the limits of this model, the measured K_{Jm} can be adjusted to K_{Jc} using the computed ratio of $[K_{CL}/K_{SSY}]$. The $[K_{CL}/K_{SSY}]$ are determined from FE calculations for the condition that $\langle A(\sigma_{22})\rangle_{CL}=A(\sigma_{22})_{SSY}$.
- For a specified specimen geometry, the $[K_{CL}/K_{SSY}]$ ratio depends on K_J,σ_y,E, the strain hardening rate (n) and σ^*. Thus, calibrating the $[K_{CL}/K_{SSY}]$ model requires measurement of both the constitutive properties of the steel and σ^*.
- The σ^* for a particular steel can be estimated by fitting a $K_{mc}(T)$ model to independent measurements of $K_{Jm}(T)$ at high levels of constraint using a procedure developed by Odette and He [14].
- The $B^{-1/4}$-type scaling of K_{Jc} derives from the $V^*=BA^*$, relation. This B-scaling is modified by use of the $K_{min}=20$ MPa$\sqrt{\text{m}}$ in ASTM E 1921.
- The $[K_{CL}/K_{SSY}]$ varies with specimen type and geometry. These effects were directly modeled, but largely derive from the effect of T-stresses. An approximate but simple treatment of T-stresses is provided by a so-called biaxiality factor β, that has been characterized for a wide range of specimen configurations [8]. Thus, overall, $[K_{CL}/K_{SSY}]$ is a function of $K_{Jm}^2/b\sigma_y,E,n,\sigma^*/\sigma_y a/W,b/B$, and β.

Figure 4 schematically illustrates the nondimensional $A(\sigma_{22})/b^2$ versus the nondimensional loading parameter, $K_J^4/(E\sigma_y b)^2$, for both SSY, where A is proportional to K_J^4, and constraint loss conditions determined by the FE crack tip field calculations. The trajectories are used to evaluate the $[K_{CL}/K_{SSY}]$ by equating the measured K_{Jm} with K_{CL} and then finding the corresponding K_{SSY}. Note, the $[K_{CL}/K_{SSY}]$ adjustment factor does not depend on the absolute value of A (or A^*), but the trajectories for constraint loss from SSY conditions do depend on σ^*.

This deterministic model can be modified to account for specimen-to-specimen statistical variations in the local cleavage fracture criteria. In this case, the local fields specify a fracture probability that varies from 0, below a threshold $K_J=K_{min}$, to a probability approaching 1 at high K_J. The ASTM E 1921 standard uses a three-parameter Weibull toughness model in which two parameters are fixed. Recently, Gao and Dodds developed a three-parameter Weibull stress model to provide $[K_{CL}/K_{SSY}]$-type constraint loss adjustments [6,7,9,15].

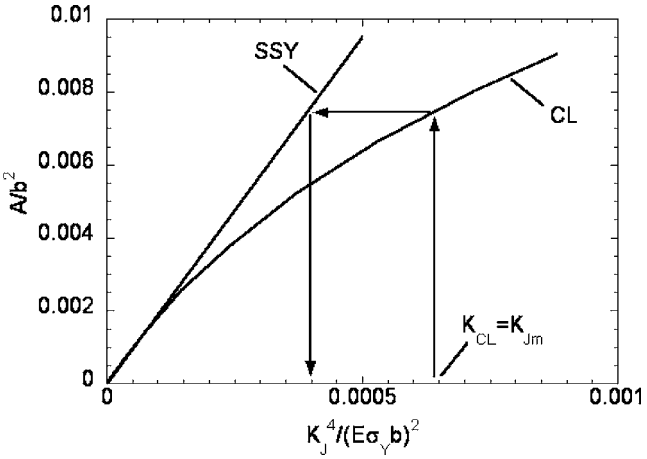

Fig. 4 Nondimensional A/b^2 versus $K_J^4/(E\sigma_y b)^2$ trajectories for SSY and constraint loss conditions from FE simulations of crack tip stress fields used to evaluate the $[K_{CL}/K_{SSY}]$ constraint adjustment factor

5 Analysis of the UCSB *b-B* Database

The UCSB *b-B* database was analyzed by sequential application of the $[K_{CL}/K_{SSY}]$ constraint loss adjustment of K_{Jm} to K_{Jc} for a specified B, followed by a $(B/B_r)^{1/4}$-K_{min} statistical size adjustment of the K_{Jc} at various B to a K_{Jr} for the reference thickness, B_r. We will call this the $[K_{CL}/K_{SSY}]$-K_{min} adjustment procedure. The effectiveness of these size adjustment procedures was evaluated by examining the degree to which the resulting K_{Jr} are size and geometry independent. In this case, the K_{Jr} should form a homogeneous population distribution, described by set statistical parameters that are consistent with expectations for cleavage toughness in the transition. This provides a physical and systematic basis to evaluate the effects of both constraint loss ($[K_{CL}/K_{SSY}]$) and corresponding contributions of statistical size scaling effects due to variations in B at high levels of constraint. Of course, these are estimates that are subject to various uncertainties associated with both limitations of the models (both constraint loss and statistical size scaling) and in the database itself. For example, an underlying assumption is that the Shoreham steel is homogeneous in its basic properties over the large region of the plate section used in this study.

A variety of approaches to this assessment were used, including statistical evaluations of the dependence of the mean, median and variance of the K_{Jr} database as a function of B and b. The procedures were also tested against independent sets of data on the Shoreham steel. These data sets include both UCSB K_{Jm} measurements on the same plate section using another set of specimens with a wide range of constraint, as well as a large data set generated by Tregoning and Joyce on other sections of plate from the Shoreham vessel (see below). Details of this analysis can be found in [6,7]. Only the key results are summarized here.

Figure 5(*a*) shows the result of adjusting the measured toughness values for constraint loss and statistical size effect using the $[K_{CL}/K_{SSY}]$-K_{min} procedure. The data have been averaged for each *b-B* combination in the database. Monte Carlo calculations show that variations of the $\langle K_{Jr}\rangle$ around an average of 91.6 ± 10.2 MPa$\sqrt{\text{m}}$ are within expected the scatter limits. The residuals, $K_{Jr}-91.6$, are shown in Fig. 5(*b*) as a function of B for all

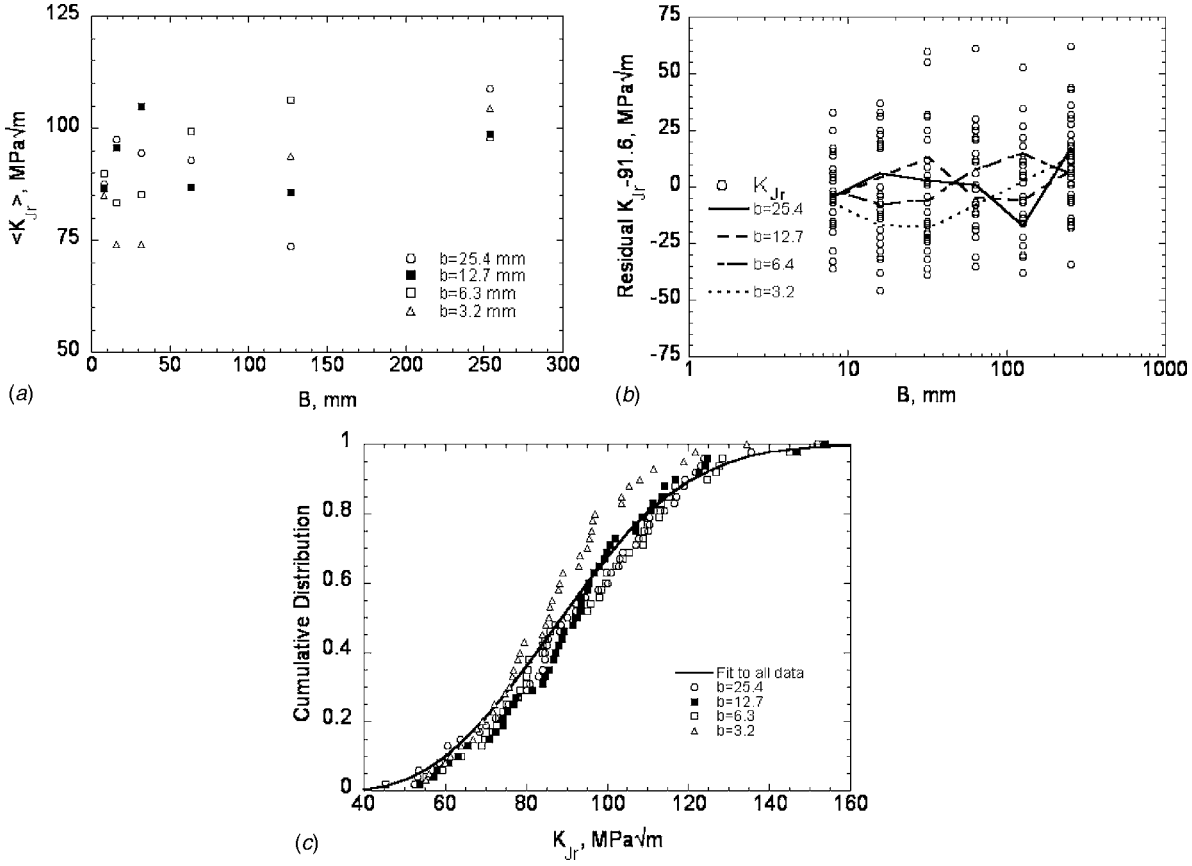

Fig. 5 (*a*) The average $\langle K_{Jr}\rangle$ versus B for the $[K_{CL}/K_{SSY}]$-K_{min} adjustment procedure. (*b*) The K_{Jr} residuals for various B. The average residuals for the various b are shown by the lines between the different B. (*c*) The cumulative distribution of the *b-B* K_{Jr} data for various b. The solid line is a fit of the data to a normal distribution function.

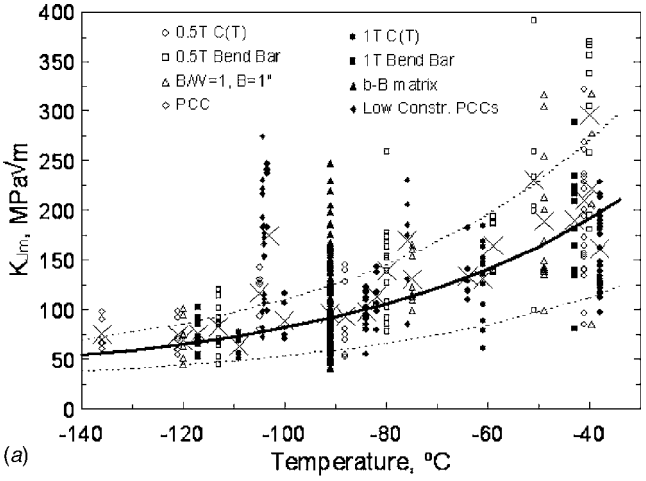

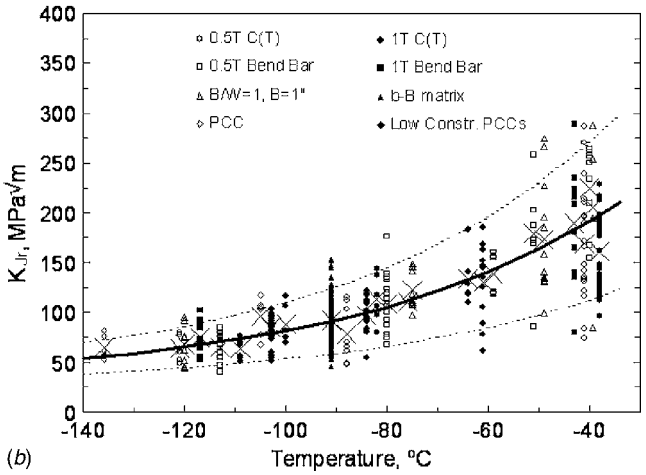

Fig. 6 The K_{Jm} (*a*) and K_{Jr} (*b*) for the UCSB *b-B* database, other UCSB data and the Tregoning and Joyce database plotted versus test temperature and the master curve for T_o=−84°C

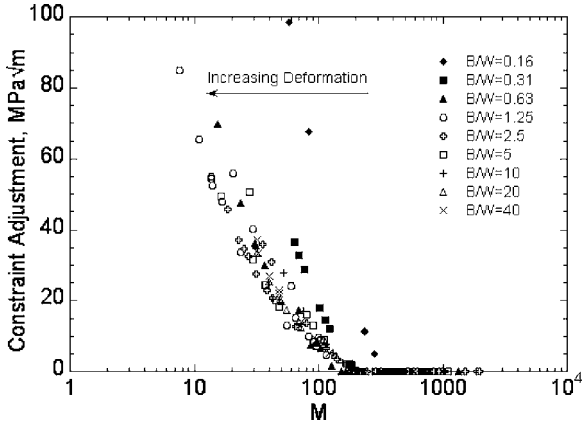

Fig. 7 Constraint loss predicted by the $[K_{CL}/K_{SSY}]$-constraint adjustment procedure as a function of *M* for the UCSB *b-B* database

b. Lines connect the average residual for a specified *b*. The residuals are reasonably distributed and centered about 0. The average residuals do not show any strong systematic trends in *b* or *B*, except at the smallest *b* and largest *B*. Close examination shows that there is a slight trend towards increasing $\langle K_{Jr}\rangle$ with increasing *b* (statistically relatively weak) and *B* (statistically weak to moderate). The averaged $\langle K_{Jr}\rangle$ for the three largest *b* are nearly identical at 93.1±9.1 MPa$\sqrt{m}$. The corresponding average is 86.3±13.1 MPa$\sqrt{m}$ for the smallest b=3.2 mm specimens. The average $\langle K_{Jr}\rangle$ for all *b* at the largest *B* is 102±20.1 MPa$\sqrt{m}$. Figure 5(*c*) shows the cumulative distribution of K_{Jr} for various *b*. Agreement is excellent for the three larger *b*, but deviates for the smallest b=3.2 mm at higher K_{Jr}. The solid line is a normal distribution fit to all the data. In addition, except for a relatively small number of data points at the highest and lowest values, the $[K_{Jr}-20]$ followed a Weibull distribution with a slope of 3.9, which is very close to the nominal value of 4. These results suggest that the $[K_{CL}/K_{SSY}]$ procedure may slightly over-adjust K_{Jm} at the smallest *b*, predicting K_{Jc} that are too low. Further, the $[B/B_r]^{1/4}$-K_{min} procedure may also slightly over-adjust K_{Jc} at the largest *B*, predicting K_{Jr} that are too high. A detailed analysis, including linear regression evaluations of the trends in *b* and *B*, suggest that the maximum over-adjustments are less than ≈10 MPa$\sqrt{m}$. The T_o for the *b-B* database averaged −84±9.3°C.

Overall, however, the $[K_{CL}/K_{SSY}]$-K_{min} adjustments result in an approximately homogeneous, well-behaved and self-consistent population of *b-B* K_{Jr} adjusted data for a remarkable range of specimen size and geometry. A corollary is that the Shoreham plate is relatively homogeneous at the 3/4-*T* location. Further support for this conclusion results from application of the $[K_{CL}/K_{SSY}]$-K_{min} procedure to the additional set of USCB K_{Jm} data. This data set includes a large number of low constraint specimens. The adjusted K_{Jr} are well represented by a master curve with the same T_o=−84°C as found for the *b-B* database. Further, the $[K_{CL}/K_{SSY}]$-K_{min} procedure was applied to the large database on other plate sections of the Shoreham vessel published by Tregoning and Joyce [16–19]. The corresponding K_{Jr} are also well represented by a master curve with a T_o of −84°C. The K_{Jm} and K_{Jr} data for the entire database (489 data points) are shown in Fig. 6 along with the master curve with T_o=−84°C.

Constraint adjustments were also carried out using a self-calibrated Wiebull stress procedure, based on a modification of the method proposed by Gao and Dodds [15]. The results are generally similar to those provided by the $[K_{CL}/K_{SSY}]$-K_{min} procedure, although the constraint adjustments are slightly larger for the Weibull stress approach [6,7].

6 Evaluation of Constraint Loss and its Potential Effects on the ASTM E 1921 T_o

Figure 7 plots the magnitude of the $[K_{CL}/K_{SSY}]$ constraint loss adjustment (i.e., without adjustment for the statistical sampling effect) for all of the measured toughness data points in the UCSB *b-B* database, grouped by common *B*/*W* ratio. At M=30 the minimum adjustment is approximately 28 MPa$\sqrt{m}$. These model based results indicate that constraint loss begins at M=100 or more and is significant at M=30, where increases in the K_{Jm} of about 20 MPa$\sqrt{m}$ or more relative to K_{Jc} can be expected.

As noted previously, the effects of constraint loss on T_o must be evaluated on a case-by-case basis. This was carried out by using the ASTM E 1921 procedure to evaluate the T_o for both the unadjusted K_{Jm} data and the corresponding $[K_{CL}/K_{SSY}]$-K_{min} adjusted K_{Jr} data. The ASTM E 1921 standard requires specimens with B/W=0.5 or 1 to ensure a high degree of lateral constraint at fracture. Thus, specimens in the *b-B* matrix with $B/W<0.5$ were not included in the T_o analysis. However, specimens with $B/W>2$ were included, consistent with the objectives of this study to evaluate statistical scaling over a wide range of *B*. Further, only data subsets that met the requirement for the minimum number of uncensored data points were analyzed and presented in the remaining results.

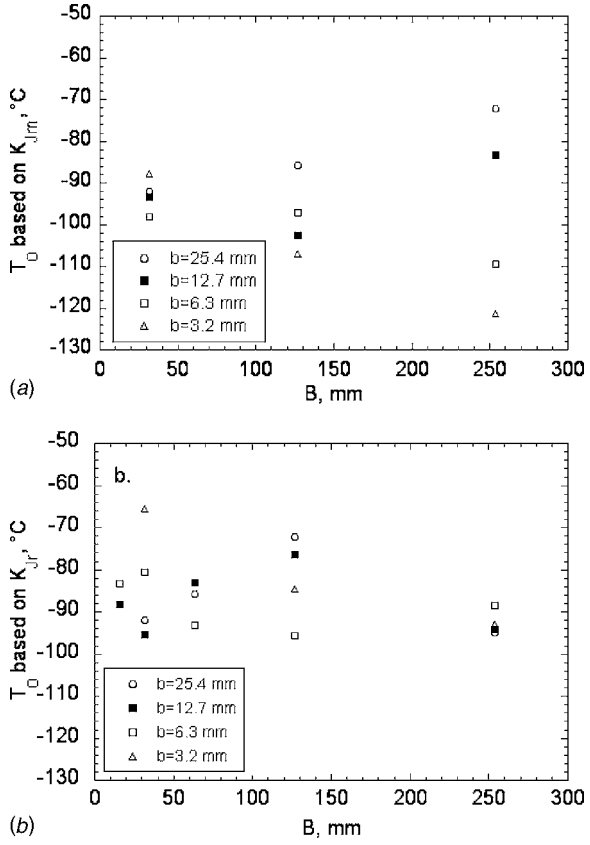

Fig. 8 (*a*) T_o determined from ASTM E1921-97 using the measured K_{Jm} data. (*b*) The T_o determined from ASTM E1921-97 using the adjusted K_{Jr} data.

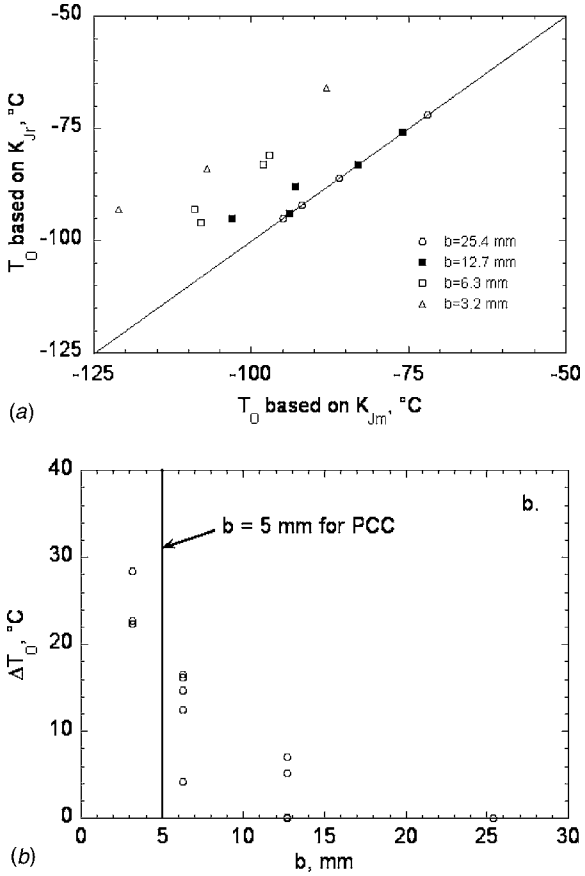

Fig. 9 (*a*) Scatter plot of T_o based on K_{Jm} versus K_{Jr}. (*b*) The T_o based on K_{Jr} minus that based on K_{Jm} versus ligament dimension, *b*.

Figure 8(*a*) plots the T_o derived from the K_{Jm} and Fig. 8(*b*) shows the corresponding T_o evaluation using the $[K_{CL}/K_{SSY}]$-K_{min} adjusted K_{Jr}. The T_o based on K_{Jm} ranging from about -70 to $-120\,^{\circ}$C with an average of approximately $-93\,^{\circ}$C. The T_o tend to be lower for the smaller b, at least at the larger B. The T_o derived from the adjusted K_{Jr} data range from about -65 to $-95\,^{\circ}$C, with an average of approximately $-84\,^{\circ}$C, or $9\,^{\circ}$C higher than the corresponding average for the unadjusted K_{Jm} data. The T_o based on K_{Jr} also follow a normal cumulative distribution with a standard deviation $\pm 9.3\,^{\circ}$C, consistent with eight tests at each *b*-*B* specimen in the matrix. A plot of the T_o from K_{Jm} versus that from K_{Jr} is shown in Fig. 9(*a*). In the seven cases for larger b, with minimal constraint adjustment, the T_o are essentially the same. However, as expected, the differences between the T_o increase at smaller b.

Figure 9(*b*) plots the difference between the T_o based on K_{Jr} versus K_{Jm} evaluations as a function of b. The line at $b=5$ mm corresponds to the pre-cracked Charpy (PCC) geometry. These results suggest that T_o calculated using the ASTM E 1921 procedure using PCC specimens may be biased by about $-15\,^{\circ}$C compared to a fully constrained SSY T_o. However, considering the possible effects of over-adjustments by the $[K_{CL}/K_{SSY}]$ procedure, perhaps a better estimate of the bias is approximately $-10\,^{\circ}$C.

Joyce and Tregoning have analyzed our data based on an alternative approach to assessing the effects of constraint loss by evaluating the effect on T_o of varying the M_{lim} from values of less than the nominal E 1921 value of 30, up to the highest value consistent with a statistically valid data subset [20]. Figure 10 shows the results of applying this procedure to the UCSB Shoreham *b*-*B* database. Here we have excluded the data for $B/b < 0.6$, since M does not properly reflect the effects of out-of-plane constraint loss for thin geometries. Figure 10(*a*) shows that T_o systematically decreases from a value of about $-85\,^{\circ}$C at $M > 300$ to approximately $-97\,^{\circ}$C at $M=30$. This is very similar to the effects of constraint loss found in our model-based analysis. Tregoning and Joyce also observed similar trends in their SEN(B) database on other plate sections of the Shoreham vessel as well as other datasets they found in the literature. These results suggest that constraint loss begins at $M \approx 200$ and T_o has a significant nonconservative bias for a M_{lim} less than about 100. These results are very similar to the effects of constraint loss found in our model-based analysis. This is demonstrated in Fig. 10(*b*) showing a T_o analysis of the fully adjusted K_{Jr} data as a function of M_{lim}. In this case $T_o \approx -86\,^{\circ}$C is approximately independent of M_{lim} even for very low values.

7 Summary and Conclusions

The results of this work can be summarized as follows:

- Both statistical stressed volume and constraint loss can play a role in the effect of specimen size on cleavage fracture toughness in the transition.
- The ASTM E 1921 statistical scaling procedure for variations in B is reasonably consistent with the UCSB *b*-*B* database trends. However, the results suggest that the $(B/B_r)^{1/4}$-K_{min} statistical size adjustment procedure slightly over predicts the effect of B variations over the very large range tested in this study. As discussed in [12] a possible reason is that there is an upper limit on B for statistical scaling.

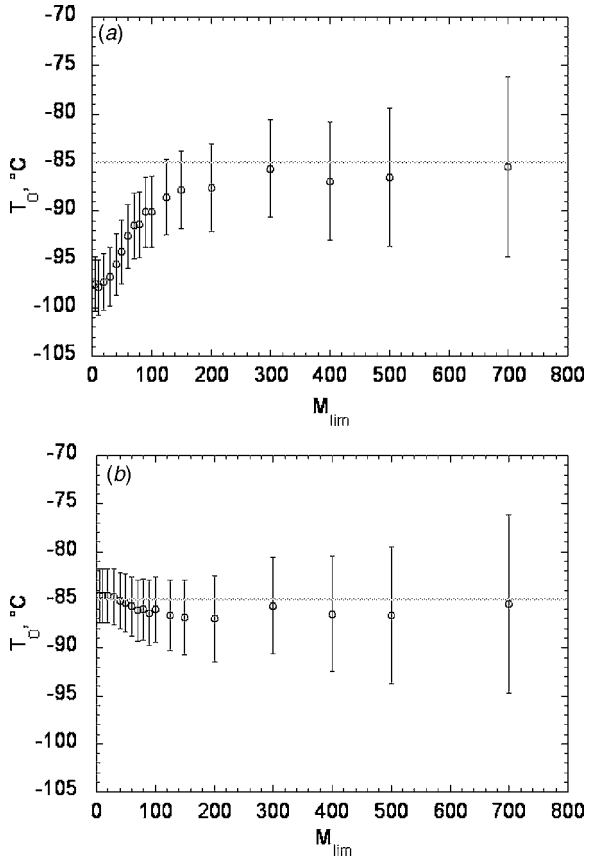

Fig. 10 Variation in T_o calculated using *a.* K_{Jm} and *b.* K_{Jr}

- For SEN(B) specimens, constraint loss begins at a deformation level specified by a value of M much higher than the value of 30 used in ASTM E 1921.
- Unrecognized constraint loss leads to a nonconservative, negative bias in the ASTM E 1921 evaluation of T_o. The quantitative effect must be evaluated on a case-by-case basis, but is estimated to be approximately $-10°C$ for pre-cracked Charpy specimens tested near the SSY T_o.
- The $[K_{CL}/K_{SSY}]$ and other similar adjustment procedures may slightly over predict constraint loss in very small specimens with low values of M.
- When used with appropriate caution, the physically based and calibrated $[K_{CL}/K_{SSY}]$-K_{min} adjustment procedures can be used to obtain good estimates of T_o for specimens that experience significant constraint loss. For example, after application of the $[K_{CL}/K_{SSY}]$-K_{min} adjustment procedure, a large database of 489 K_{Jr} on Shoreham steel were reasonably represented by a single master curve with $T_o \approx -84°C$. As a final note in proof, recently, a similar $[K_{CL}/K_{SSY}]$-K_{min} analysis of a tempered martensitic steel also resulted in a self-consistent set of K_{Jr} data with a common $T_o = -98°C$ [21].

Acknowledgment

This work was primarily funded by U.S. Nuclear Regulatory Commission (NRC) Contracts No. NRC-04-94-049 and NRC-04-01-064. We give special thanks to Robert Tregoning, previously at the Carderock Division Naval Surface Warfare Center, and more recently at the US NRC. Rob's helpful advice and insightful comments, as well as his generous assistance in both the testing at Carderock and in providing his outstanding database, were key elements in completing this work. The encouragement and support of our NRC project monitors, the late Mike Vassilaros, who helped us to initiate this project, and more recently Carolyn Fairbanks and Tanny Santos, were critical to our effort. Funding for much of the FE modeling was provided by the U.S. Department of Energy Grant No. DE-FG03-87ER. The authors also gratefully acknowledge Joe Waskey at Carderock and Tom Huang and Won Jon Yang UCSB for their assistance in some of the testing and data evaluations. The always generous support and numerous helpful suggestions of many members of the UCSB Materials Performance and Reliability Group are also much appreciated.

Nomenclature

A = computed area inside a σ_{22} stress contour
A^* = critical area for cleavage for the σ^* contour.
a = crack length
B = crack front length (thickness)
B_r = reference crack front length (B_r=25.4 mm)
b = ligament dimension
E = Young's modulus
K_{CL} = K_{Jm} with constraint loss
K_J = elastic-plastic applied loading parameter based on the J-integral = $\sqrt{(EJ)}$
K_{max} = maximum measurable K_{Jm} in ASTM E 1921-97
$K_{mc}(T)$ = fracture toughness master temperature curve
K_{min} = minimum K_J for cleavage fracture
K_{Jm} = measured elastic-plastic toughness
K_{Jc} = fracture toughness adjusted to SSY
K_{JB} = K_{Jm} adjusted to the reference thickness using the $[B/B_r]^{1/4}$-K_{min} statistical size adjustment procedure (but not adjusted for constraint loss).
K_{Jr} = K_{Jm} adjusted to K_{Jc} with the $[K_{CL}/K_{SSY}]$ procedure for constraint loss and then adjusted to K_{Jr} with the $[B/B_r]^{1/4}$-K_{min} statistical size adjustment procedure.
K_{SSY} = small scale yielding equivalent K_J
M = nondimensional deformation parameter $K_{Jm}^2/(E\sigma_y b)$
M_{lim} = minimum censoring M (=30)
M_{nom} = M for a specified toughness
M_{av} = average M for a subset of data
n = strain hardening exponent
p = power law fit parameter
S = loading span
T = temperature
T_o = master curve temperature at a median toughness of 100 MPa$\sqrt{}$m
V = computed volume inside a σ_{22} stress contour
V^* = critical volume for cleavage for the σ^* contour
W = specimen width
σ_{22} = stress component normal to the crack plane
σ^* = critical local σ_{22} stress for cleavage
σ_y = yield strength
SEN(B) = single edge notch bend fracture toughness specimen
$C(T)$ = compact tension fracture toughness specimen
SSY = small scale yielding
CL = constraint loss
$<>$ = average value of a quantity

$[K_{CL}/K_{SSY}]$ = computed ratio of applied K_J for constraint loss and SSY conditions to achieve the same stressed A

$[B/B_r]^{1/4}$-K_{min} = statistical size adjustment procedure in E 1921-97

$[K_{CL}/K_{SSY}]$-K_{min} = the combined constraint loss and statistical size adjustment procedure

References

[1] American Society for Testing and Materials, 1998, *E 1921-97 Standard Test Method for Determination of Reference Temperature, T_o, , for Ferritic Steels in the Transition Range*, ASTM, West Conshohocken.

[2] Merkle, J. G., Wallin, K., and McCabe, D. E., 1998, *Technical Basis for an ASTM Standard on Determining the Reference Temperature, T_o, for Ferritic Steels in the Transition Range (NUREG/CR-5504, ORNL/TM-13631)*, U.S. Nuclear Regulatory Commission, Washington.

[3] Electric Power Research Institute, 1998, *Application of Master Curve Fracture Toughness Methodology for Ferritic Steels*, EPRI Report TR-108390, Palo Alto.

[4] Wallin, K., Saario, T., and Törrönen, K., 1984, "Statistical Model for Carbide Induced Brittle Fracture in Steel," Met. Sci., **18**, pp. 13–16.

[5] Nevalainen, M., and Dodds, R. H., Jr., 1995, "Numerical Investigation of 3D Constraint Effects on Brittle Fracture in SE(B) and C(T) Specimens," Int. J. Fract., **74**, pp. 131–161.

[6] Rathbun, H. J., Odette, G. R., He, M. Y., Lucas, G. E., and Yamamoto, T., 2006, "Size Scaling of Cleavage Toughness in the Transition: A Single Variable Experiment and Model Based Analysis (NUREG/CR-6790)," U.S. Nuclear Regulatory Commission, Washington.

[7] Rathbun, H. J., Odette, G. R., He, M. Y., and Yamamoto, T., 2006, "Influence of Statistical and Constraint Loss Size Effects on Cleavage Fracture Toughness in the Transmission-A Model Based Analaysis," Eng. Fract. Mech. (to be published).

[8] Anderson, T. L., 1995, *Fracture Mechanics Fundamentals and Applications*, CRC Press, Boca Raton.

[9] Petti, J., and Dodds, R. H., Jr., 2004, "Constraint comparisons for common fracture specimens: C(*T*)s and SE(*B*)s" Eng. Fract. Mech., **71**(18), pp. 2677–2683.

[10] Rathbun, H. J., Odette, G. R., and He, M. Y., 2000, "Size Scaling of Toughness in the Transition: A Single Variable Experiment and Data Base Assessment," *Proceedings of the ASME PVP 2000*, ASME, New York, 412, pp. 113–124.

[11] Rathbun, H. J., Odette, G. R., and He, M. Y., 2001, "On the Size Scaling of Cleavage Toughness in the Transition: A Single Variable Experiment and Model Based Analysis," *Proceedings of the International Congress on Fracture 10*, CD-ROM format.

[12] Rathbun, H. J., Odette, G. R., Yamamoto, T., and Lucas, G. E., 2006, "Influence of Statistical and Constraint Loss Size Effects on Cleavage Fracture Toughness in the Transition-A Single Variable Experiment and Database," Eng. Fract. Mech. **73**(1), pp. 134–158.

[13] Hibbit, Karlsson and Sorenssen, Inc., 1998, ABAQUS Users Manual 5.8.

[14] Odette, G. R., and He, M. Y., 2000, "A Cleavage Toughness Master Curve Model," J. Nucl. Mater., **283**, pp. 120–127.

[15] Gao, X., Ruggieri, C., and Dodds, R. H., Jr., 1998, "Calibration of Weibull Stress Parameters Using Fracture Toughness Data," Int. J. Fract., **92**, pp. 175–200.

[16] Joyce, J. A., and Tregoning, R. L., 2001, "Effects of Material Inhomogeneity on the T_o Reference Temperature in Thick Section A533B Plate," *Proceedings of the ASME PVP 2001*, ASME, New York, 423, pp. 157–165.

[17] Joyce, J. A., and Tregoning, R. L, 2001, "Development of the T_o Reference Temperature From Precracked Charpy Specimens," Eng. Fract. Mech., **68**(7), pp. 861–894.

[18] Tregoning, R. L., and Joyce, J. A., 2000, "T_o Evaluation in Common Specimen Geometries," *Proceedings of the ASME PVP 2000*, ASME, New York, 412, pp. 143–152.

[19] Tregoning, R. L., and Joyce, J. A., 2002, "Application of a T-Stress Based Constraint Correction to A533B Steel Fracture Toughness Data," ASTM Special Technical Publication n. 1417, pp. 307–327.

[20] Joyce, J. A., and Tregoning, R. L., 2005, "Determination of Constraint Limits for Cleavage Initiated Toughness Data," Eng. Fract. Mech., **72**(10), pp. 1559–1579.

[21] Odette, G. R., Yamamoto, T., Kishimoto, H., Sokolov, M, Spätig, P., Yang, W. J., Rensman, J.-W., and Lucas, G. E., 2004, "A Master Curve Analysis of F82H Using Statistical and Constraint Loss Size Adjustments of Small Specimen Data," J. Nucl. Mater., **329-333**(2), pp. 1243–1247.